Growth of Bi2Te3 Nanowires for Use in Nonlocal Photocurrent Generation

Luc Nguyen[1,2] and Dong Yu[2]

[1] *University of California, Berkeley, Department of Physics,*

[2] *University of California, Davis, Department of Physics and Astronomy*

(Dated: December 22, 2024)

Topological insulators such as Bi_2Se_3 and Bi_2Te_3 have demonstrated themselves to be platforms for exciting and novel physics. In particular, in previous studies we have observed millimeter scale non-local photocurrent in Bi_2Se_3 that we believe is a direct consequence of exciton formation. ARPES data also indicates exciton formation [1] in Bi_2Te_3, which suggests similar photocurrent experiments could be carried out on Bi_2Te_3. In this paper, I have developed a recipe to grow Bi_2Te_3 nanowires using a vapor-liquid-solid (VLS) chemical deposition process in order fabricate devices for such experiments.

I. INTRODUCTION

Topological materials are a topic of interest primarily due to their topological surface states (TSS), which are topologically protected against defects. In order to progress in developing any applicable technologies with these materials, a greater understanding of their underlying properties must be gained. We are particularly interested in the topological insulators (TIs) Bi_2Se_3 and Bi_2Te_3. Using scanning photocurrent microscopy (SPCM), we are able to gain insight into the electronic properties of these materials.

In particular, previous experiments in our group have demonstrated millimeter scale non-local photocurrent[2] in Bi_2Se_3 nanowires, which we believe is due to the formation of a TSS exciton condensate. Previous time-resolved angle-resolved photoemission spectroscopy (trARPES) data indicates similar exciton formation[1], except with the electron in a hybridized TSS-bulk state and the hole in a bulk state. This spatial separation between the electron and the hole would likely result in a longer excitonic lifetime which could be measured experimentally. To carry out this experiment, we must first create the necessary Bi_2Te_3 devices. In this paper, I will discuss the mechanisms behind our observed nonlocal photocurent as well as the recipe developed for creating Bi_2Te_3 nanowires.

II. TOPOLOGICAL INSULATORS

Topological insulators are similar to trivial insulators in that their insulating properties stem from a gap between the conduction and valence band. However, strong spin-orbit coupling (SOC) causes a band inversion; the states that would be at the bottom of the conduction band without SOC are shifted to the top of the valence band, and the states that would be at the top of the valence band are shifted to the bottom of the conduction band. For this band structure to transform back into a trivial insulator, the bands must come into contact and "untwist", resulting in a conducting state. As a result, on the boundary between the insulating states in the bulk and the trivial insulating states of individual particles, there must be conducting states known as the bulk boundary correspondence. This is what provides topological insulators their defining property of having conducting surface states and insulating bulk states.

The surface states of TIs exhibit linear dispersion near their Dirac point. Similar to graphene, this property leads TSS carriers to act as massless fermions. Materials with such linear dispersion have been theorized to support exciton condensation [3]. The coupling between the electrons and the holes is then $\alpha = \frac{e^2}{\kappa \hbar v_f}$, where e is the fundamental charge, κ is the dielectric constant, and v_f is the Fermi velocity. This coupling constant compares the Coulomb interaction with the kinetic energy, and is enhanced for materials with small κ and small v_f. Although TIs have bigger dielectric constants compared to graphene, they have a smaller Fermi velocity which compensates and results in an α on the order of 10^{-1} [4]. This high coupling, combined with their demonstrating long lifetime of transient states and fairly high critical temperatures (around 30 K) suggests that TIs have a strong potential to achieve exciton condensation.

III. NONLOCAL PHOTOCURRENT MEASURMENTS

In SPCM, a laser beam is raster-scanned over an area and the current generated from each point measured. In a normal semiconductor in the absence of any external

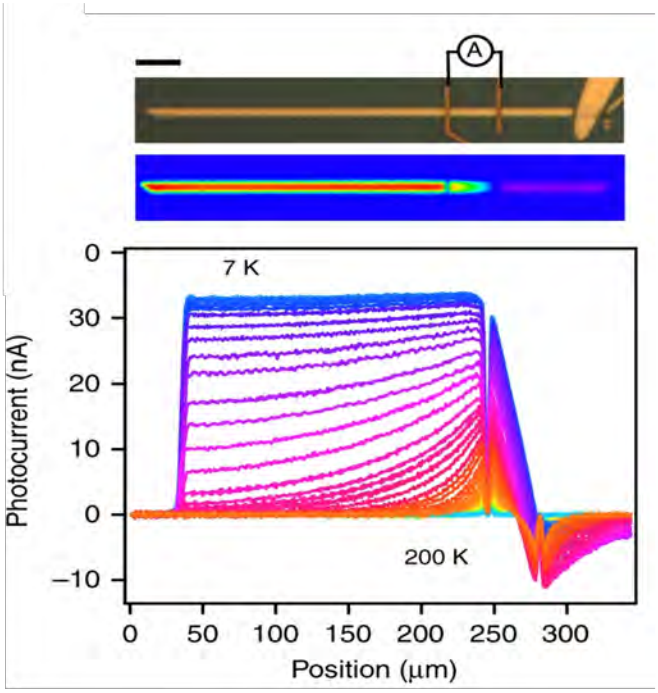

FIG. 1: Results of SPCM on Bi_2Se_3, sourced from [2]. At low temperatures, photocurrent has little decay with distance, but decays with greater strength at higher temperatures.

electric field, one would expect any current to come from minority free carriers [5] excited either by the laser photons or by the temperature increase caused by the laser. Such free carriers would then travel diffusively leading to an exponential decay in current with distance with characteristic length $L_d = \sqrt{D\tau}$, where D is the diffusion constant and τ is the lifetime of minority carriers. However, our SPCM measurments on the TI Bi_2Se_3, visualized in Fig 1 seem to have little to no decay at low temperatures. With the observed decay lengths and τ (found using transient photocurrent measurements), the diffusion constant would have to be multiple orders of magnitude greater than highest reported for TIs. We believe that this observed lack of decay, which we refer to as nonlocal photocurrent, is caused by the formation of an exciton condensate in our device, visualized in Fig 1.

IV. INDIRECT EXCITONS

TIs are uniquely well suited for nonlocal photocurrent measurements. Due to the spin momentum locking [6], scattering off of non-magnetic impurities is suppressed. Similarly due to the charge neutrality of excitons, scattering off of monopole charge impurities is supressed as well. By examining exciton formation more closely, we

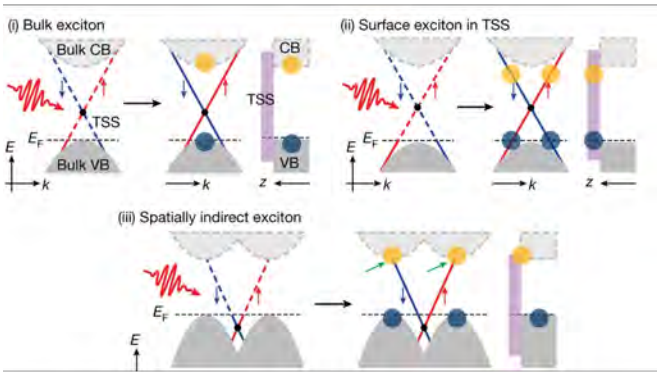

FIG. 2: Momentum- (left) and real- (right) space representations of (i) bulk excitons in a topological insulator, (ii) surface excitons in a topological insulator and (iii) a spatially indirect excitonic topological insulator system. Yellow and navy dots represent electron–hole pairs. Sourced from [1]

find that Bi_2Te_3 is a particularly good candidate for nonlocal photocurrent measurements due the spatially indirect nature of its excitons.

In TIs, exciton formation can fall into three different categories. The electron and hole can both exist in the bulk, both in the surface, or one in each. In the first case, displayed in Fig 2 (i), the exciton has similar characteristics to those observed in conventional semiconductors. The second case, visualized in Fig 2 (ii) is more similar to graphene, and could have interesting applications due to its linear dispersion. Indeed, due to its band structure, we believe that the excitons observed in Bi_2Se_3 are of this variety. The third is the scenario we are now intersested in, and occurs when the excitonic state exists at the bulk-surface mixing point (green arrows in Fig 2 (iii)) and the TSS hybridizes with the bulk wavefunction.This state provide a unique scenario where the electron and the hole are spatially separated, while still retaining a low effective mass. This variety of exciton is referred to as a spatially indirect exciton. Due to the spatial separation, this variety has a particularly long lifetime in comparison to the other two. Recent trARPES [1] displayed in Fig 3 indicates that p-type Bi_2Te_3 can support indirect excitons, implying that it might be capable of similar but distinct nonlocal photocurrent measurements as Bi_2Se_3.

V. GROWTH OF SAMPLES

We used an Au catalyst-assisted vapor-liquid-solid method to grow the Bi_2Te_3. This method involves coating the substrate in 10 nm of Au before performing chemical vapor deposition. Direct deposition from vapor onto solid is a slow process; instead, we have our vapor first

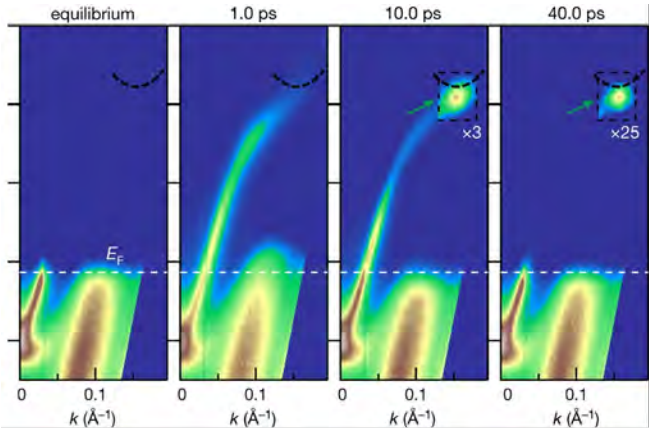

FIG. 3: trARPES data for hole doped Bi_2Te_3. trARPES spectra along the $\bar{\Gamma} - \bar{M}$ direction for a p-type sample with E_F=0.09eV before pumping. Dashed black line represents the bulk conduction band. As the system relaxes after the pump, there is a build up indicative of indirect excitons. Sourced from [1]

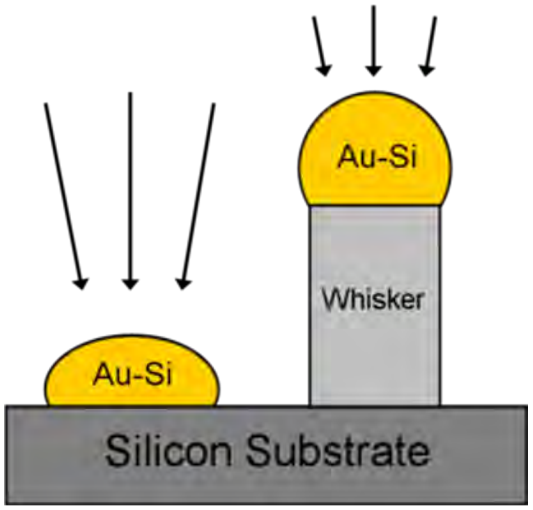

FIG. 4: In VLS, vapor is first adsorbed onto catalyst particles before precipitating out into nanostructures. Sourced from [7].

mix with gold catalyst particles, before being precipitated out, visualized in Fig 4.

This two step process requires less energy than direct from vapor to solid, increasing deposition time. Most importantly, the gold provides prefer deposition sites, allowing for distinct structures such as nanoplates or our desired nanowires. Our setup is visualized in Fig 5. Our precursor was placed at the center of a quartz tube on top of a thermal couple, while our substrate, a 10 nm Au-coated silicon between 2-5 cm in length, was placed downstream. The tube was then heated in a furnace, and Argon gas flowed through the tube to carry vapor to the substrate. In all attempted growths, a precursor

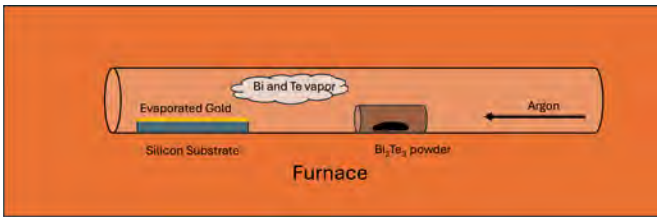

FIG. 5: The setup used for growth. A quartz tube with the precursor in the center and the 10 nm Au coated Si substrate downstream was heated up in a furnace. Argon was flowed through to carry vapor to the substrate.

of 5N (99.999 %) purity Bi_2Te_3 powder was used, which was sourced from Thermo Fisher Scientific. The tube was baked at 1000 °C and cleaned using IPA and acetone after each use, and was flushed with argon 3 times before each growth. Temperature, Argon flow rate, and position of the substrate were all varied in order to find optimal growth conditions. Growth results were first inspected under an optical microscope to assess morphology. If there was a reasonable amount of crystalline or other interesting structures, the growth was examined using a scanning electron microscope (SEM). This provided a closer look at the morphology as well as seeing the locations of individual gold particles. Using the SEM, we could also perform Energy-dispersive X-ray spectroscopy (EDS) to determine the stoichiometry of each structure.

VI. RESULTS

We found that our best growth conditions were at 590 ±10 °C using 190 ±10 mg of Bi_2Te_3, with substrate distance of 12 cm from the center and with argon flow rate of 50 ±10 sccm (standard cubic centimeter per minute), grown for 10 hours. In these conditions, nanowires of approximately 50:50 Bi to Te were observed, with some having the 40:60 ratio indicative of Bi_2Te_3. The ratios of Bismuth to Tellurium were determined using EDS.

At these temperatures it was also found that, between approximately 9 and 14 cm from the center, stoichiometry was largely consistent and only morphology differed. Between 590 °C and 620 °C seemed to consistently maintain an approximately 50:50 Bi to Te ratio, with fluctuations throughout the substrate. Below 590 °C only amorphous structures seemed to be grown, likely due to very low amount of melting of the precursor (Bi_2Te_3 has a melting point of 685 °C). Above 620°C, higher temperatures resulted in less and less Te deposition. By 680 °C, nearly only Bi is deposited, as is visualized in Fig 7. Near the gold particles at these high temperatures EDS

(a)

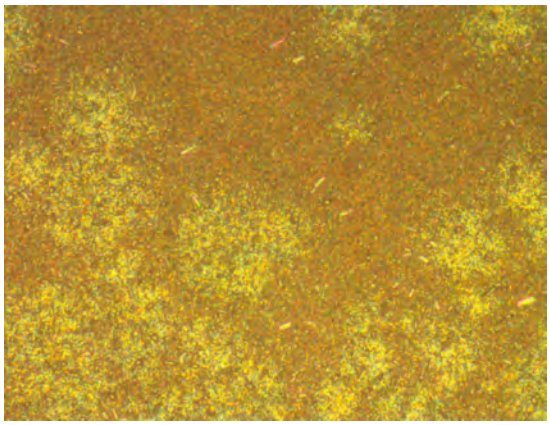

(b)

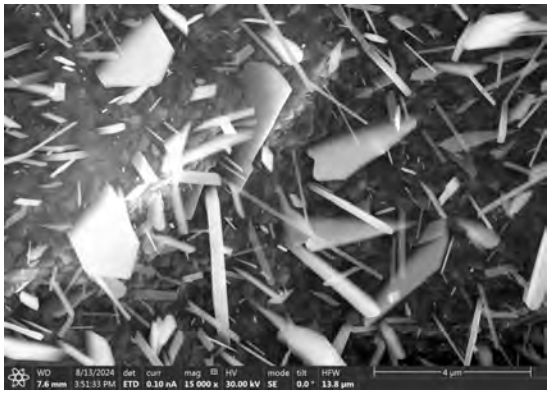

FIG. 6: (a) Real space image of growth at 590 °C, with 50 sccm and distance of 12 cm from furnace center. Noticeably only sparse wires are visible and reflective. (b)SEM of the same growth. There is a high density of nanowires and nanoribbons.

indicates there is around a 60:40 Bi to Te ratio. Since the deposition comes out from the gold, this indicates that the most recent precipitation had more Te; this was likely occurring while the furnace was cooling down. Growths were also attempted at vacuum but produced too low yield to gather any useful data for optimal growth or to eventually fabricate devices.

VII. CONCLUSION AND FUTURE WORK

In summary, topological insulators like Bi_2Te_3 and Bi_2Se_3 present the potential to realize long-distance excitonic transport. Due to their linear dispersion, excitons in these materials have extremely low effective mass. Bi_2Se_3 has already demonstrated nonlocal photocurrent measured via SPCM, with characterstic length far greater than could be achieved with free minority carriers. In addition, ARPES data indicates Bi_2Te_3 could support spatially indirect excitons, which theory suggests could have even greater efficacy of transport due to their longer lifetime. We have determined the conditions needed to grow Bi_2Te_3 nanowires in order to begin experiments to confirm this property. In the future, the addition of more Te precursor could lead to larger wires more conducive to device fabrication, and Se will likely need to be added to achieve proper p-type doping. The next step is to fabricate devices and carry out SPCM measurements to further investigate Bi_2Te_3 potential as a exciton transport platform.

(a)

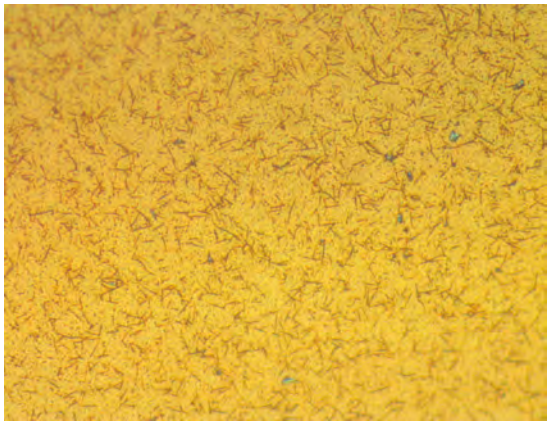

(b)

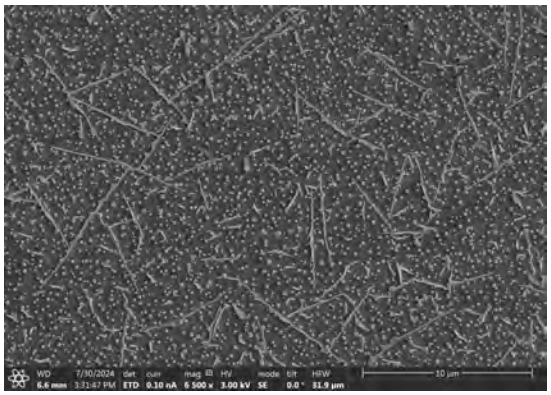

FIG. 7: (a) Real space image of growth at 700 °C at 100 sccm, 9 cm from center. High density of what seems like hair-like wires.(b) SEM image of the same growth. While EDS indicates the ridges are mostly pure Bi, near the gold particles there is a 60:40 Bi to Te ratio.

[1] R. Mori, S. Ciocys, K. Takasan, P. Ai, K. Currier, T. Morimoto, J. Moore, and A. Lanzara, Spin-polarized spatially indirect excitons in a topological insulator, Nature **614**,

249 (2023).
[2] Y. Hou, R. Wang, R. Xiao, L. McClintock, H. Clark Travaglini, J. Paulus Francia, H. Fetsch, O. Erten, S. Y. Savrasov, B. Wang, A. Rossi, I. Vishik, E. Rotenberg, and D. Yu, Millimetre-long transport of photogenerated carriers in topological insulators, Nature Communications **10**, 5723 (2019).
[3] C. Triola, A. Pertsova, R. S. Markiewicz, and A. V. Balatsky, Excitonic gap formation in pumped dirac materials, Phys. Rev. B **95**, 205410 (2017).
[4] C. Triola, A. Pertsova, R. S. Markiewicz, and A. V. Balatsky, Excitonic gap formation in pumped dirac materials, Phys. Rev. B **95**, 205410 (2017).
[5] R. GRAHAM and D. YU, Scanning photocurrent microscopy in semiconductor nanostructures, Modern Physics Letters B **27**, 1330018 (2013), https://doi.org/10.1142/S0217984913300184.
[6] M. Kohda, T. Okayasu, and J. Nitta, Spin-momentum locked spin manipulation in a two-dimensional Rashba system, Scientific Reports **9**, 1909 (2019).
[7] Wikipedia, enVapor–liquid–solid method (2024), page Version ID: 1232372475.